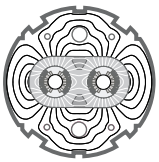

LHC Project Note 213

2000-03-30

Ana.Arauzo.Garcia@cern.ch

Computer simulation of Beam Loss Detection in the Arcs of the LHC

Author(s) / Div-Group:Ana Arauzo Garcia, Claude Bovet / SL-BI

Keywords: Beam loss, radiation protection

Abstract

A loss detection system is proposed here for the arcs of LHC. The detectors will be placed outside the cryostat along the short straight sections. The main problem is to evaluate the radiation produced at the detectors as a function of the proton loss. This has been done with a detailed 3-D geometry of the half-cell and a Monte Carlo simulation of the shower computed by the code GEANT 3.21 [1]. The results show a complete independence of losses in both beam and determine the exact positions for the loss detectors.

1. Introduction

There have been several reports of estimations of dose levels due to beam losses and beam gas interactions [2,3,5,6,7].

The Monte Carlo shower code GEANT 3.21 has been used to simulate the impact of high energy protons (point losses) on the aperture of superconducting magnets in the LHC arcs. These calculations allow to determine the sensitivity of beam loss monitors for the LHC as well as the suitable position and number of these monitors.

At top energy, the number of lost protons that lead to a magnet quench has been obtained to be, for medium range losses, of about 10^7 lost protons per meter. A loss detection system must be sensitive to much smaller losses to prevent quenches.

The geometry used in the simulations contains the Short Straight Section (SSS) with a twin-aperture quadrupole, two octupoles, and two combined sextupole-dipole correctors (MSCB), as well as surrounding dipoles plus correctors.

The protons hit the beam screen at a maximum value of the horizontal or vertical beam envelope. The incident proton interacts with a nucleus from the beam screen or other material, beam pipe or coil. The resulting hadronic shower is accompanied by an electromagnetic shower. GEANT 3.21 uses by default GHEISHA to describe hadronic interactions.

As the shower develops through the magnet material, the produced particles lose energy in inelastic interactions with atoms along their track. The distribution of these energy losses along the shower is strongly correlated to the number of secondaries, which is maximum at a certain distance of the incidence point. That distance depends on the energy of the incident proton as well as on the radiation length and the hadronic absorption length of the material.

Detectors outside the vacuum vessel have the advantage of easier accessibility and

positioning flexibility. Furthermore there are far less restrictions on the size of the detector.

2. Location of losses

In the LHC the bending field needed to guide the top energy 7 TeV protons is of about 8.3 tesla. This field is reached by superconducting magnets operating at a nominal current of 11.8 kA in the most recent design. Due to the enormous energy stored in the main dipole and quadrupole magnets, fast and efficient beam loss monitors are required to avoid damages caused by beam losses on these superconducting magnets. Quench levels have been computed for different loss durations [3]. For a medium range loss (lasting 10 milliseconds) the number of lost top energy protons which induces a quench in the magnet is of the order of 10^7 (for local or for distributed losses). At injection energy quenching is produced with 10^9 loss protons. A loss detection system must be able of detecting much smaller losses than that required to prevent quenches in both beams.

The beam loss monitors layout must be designed analysing where the losses can happen. During the beam lifetime, the losses are concentrated in the cleaning sections, where a two-stage collimation system catches most of the primary and secondary halo. Beyond the cleaning sections, there are still some protons whose betatronic amplitude is wider than the aperture of the ring, forming what is called the tertiary halo. These protons will therefore be scraped by the bottlenecks of the beam screen. Along a cell, aperture limitations are located near the quadrupoles where the betatronic functions have a maximum value. The absolute position of a quadrupole combined with the local amplitude of the closed orbit will define the likely vacuum chamber bottlenecks. There are also some possible misalignments between the end of a quadrupole and the adjacent dipoles. The accuracy of alignment gives a displacement of the beam screens by a maximum of 3 mm peak to peak from one magnetic element to the next. It has been shown [4] that most losses will happen on the first half of the quadrupole and misalignments can produce losses in the upstream dipole or in the downstream one.

We have considered these three possible locations of the losses. To find the longitudinal distribution of secondaries outside the cryostat, simulations of the shower developing down-stream have been done with the program GEANT. In this way, we can obtain the best positions of the loss detectors for every quadrupole in a half-cell, and evaluate a proposal for the beam loss detector layout.

The losses produced by protons hitting the beam screen in the arcs half-cells are distributed in a few meters in the quadrupole or in the upstream dipole [4]. The loss distribution spreading depends on the limitation in aperture, or tertiary halo width and the misalignment between the beam screens of the different magnetic elements. We admit the case of a tertiary halo effective width of 1 mm [4] and an incident betatronic angle of 0.25 mrad at the location of impact. In this case, losses happen from -400 to 0 cm in the quadrupole, from -700 to –325 cm in the upstream dipole for a misalignment of more than 1 mm; and at +325 cm in front of the downstream dipole for a misalignment of more than 0.6 mm.

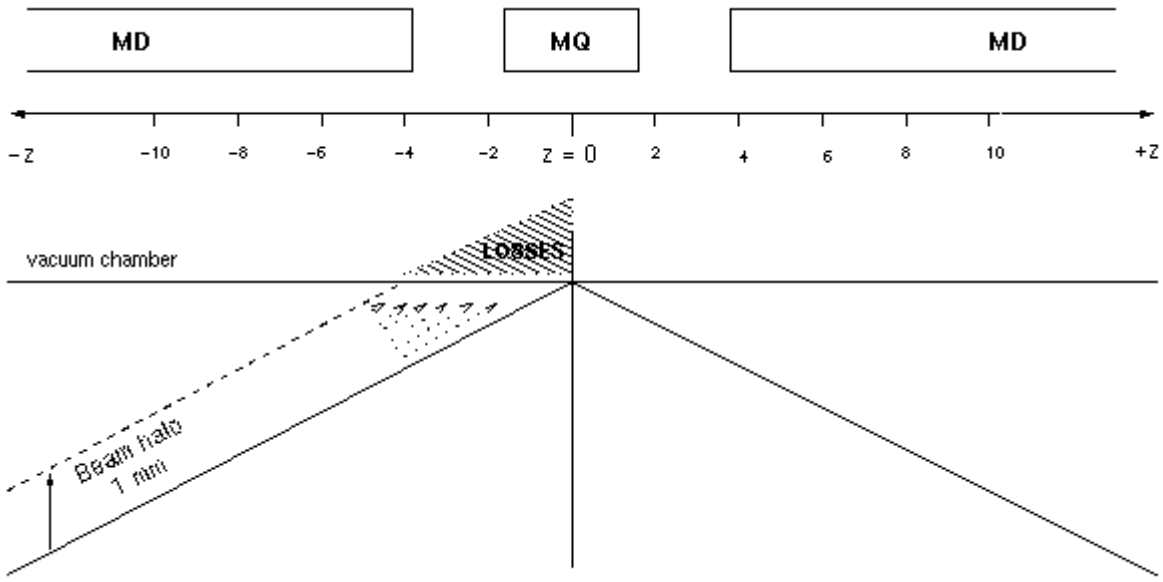

Fig. 1. Beam loss in the Main Quadrupole (MQ) for a perfect alignment of both Main Dipoles (MD). The beam goes in the +z direction. The striped triangle represents the distributed loss for a beam halo width of 1 mm. The scale in the z axis is in meters.

The shape of the loss distribution is related to the distribution of the scraped protons in the so-called tertiary halo. The beam halo is the tail of the bunch transversal distribution. We may consider a linear dependence for the distribution of losses in the most likely points in the arcs.

In the simulation of the losses, we have evaluated the effect of a point loss of one proton in a point. To have an idea of the effect of a distribution loss, in some of the cases considered, a complete set of point losses have been calculated and then integrated over the distribution loss extension. We will see that, the evaluation of a point loss is a good approximation for a distribution loss.

For quench control we must be able of detecting the developed hadronic and electromagnetic shower caused by a point loss. The quench level for a 10 ms transient loss is of the order of 10^7 protons [3].

3. Geometry and Procedure

The geometry used in the simulations corresponds to a Short Straight Section (SSS) of the LHC arcs. The layout and the different elements configuration and description is based mainly on *ref. 8*, as well as the latest modifications when available. The original design has been taken from T. Spickerman calculations [2]. However, some important modifications have been made in the geometrical set-up, materials and magnetic field configuration in the main magnets.

The code GEANT 3.21 calculates the hadronic and electromagnetic cascade produced by the interaction a beam proton hitting the beam screen at a determined longitudinal position. This is what is called a ‘point loss’. Most simulations have been done with a point-loss of

protons. As stated above, in some particular cases, loss distributions have been integrated to give the developed shower for a longitudinal loss distribution.

We are interested in the detection of losses outside the cryostat. Loss detectors like PIN diodes are sensitive to the passage of Minimum ionising particles (MIPs). Therefore, we are going to analyse the number of secondaries reaching a detector placed outside the vacuum vessel.

3.1. LHC half-cell

The SSS of the half-cell consists of a main twin aperture quadrupole (MQ), and the surrounding main bending magnets plus correctors. In the geometry used, we are centred on the MQ, and only the MD first neighbours, plus the corresponding corrector magnets, are defined. The corrector magnets are the following: two octupoles (MO) and two combined sextupole-dipole correctors (MSCB) for the MQ, and two decapoles (MDc) together with two sextupoles (MS) for every MD. The geometry has been simplified to avoid an excessive number of interfaces, which would enormously complicate the program handling and increase the computing time.

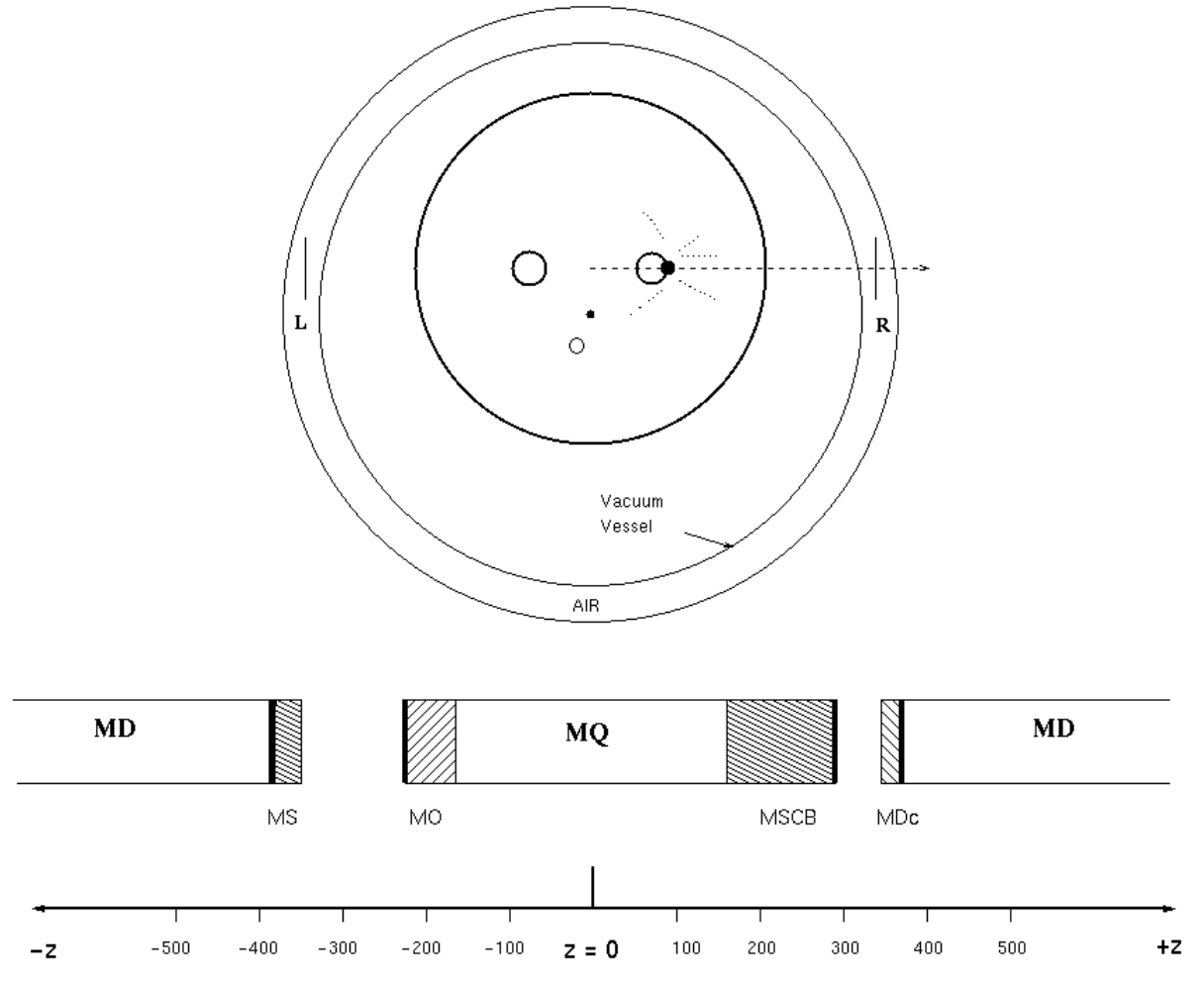

Fig. 2. Detail of the SSS half-cell geometry simulated. Top: cross-section which shows the beam pipes, cryostat and loss detectors (L, R). Bottom: longitudinal configuration, including the quadrupole (MQ), the dipoles (MD) and correctors (z values are in centimeters).

In Fig. 2 is plotted the geometrical configuration for the LHC half-cell. In the top of it, the cross section shows the beam pipes and the cryostat, together with the position of a point loss and the detectors, L, for the left detector and R, for the right detector. In the bottom of the figure, the longitudinal section is plotted, with the magnets configuration and the intermagnet gaps.

To obtain the number of particles going out of the vacuum vessel, two theoretical loss detectors have been placed outside the cryostat, on both sides, all along the longitudinal geometrical configuration. These are in an air medium to reproduce real conditions. For that, it has been defined a detection cylinder surrounding the cryostat and filled with air. Both loss detectors consist of an aluminium foil with the following dimensions: thickness = 0.05 cm, height = 10 cm and length = 3600 cm. In the cross-section view of the beam (see Fig. 2 top), the geometric configuration contains a detector at the right foreseen for the right beam, and a detector at the left, foreseen for the left beam. For every point loss, the generated particles are counted in both detectors.

3.2. Magnetic fields

The values for the bending field in the MD and the focalising field in the MQ are given from an external file to the main program. This allows to take into account the effect of the magnetic field while the tracking of the particles in the magnetic media. The magnetic field data are obtained with the program ROXIE for a nominal beam at 7 TeV in one of the quadrant of every magnet. The field is mapped in Cartesian co-ordinates, by steps of 1 mm, from the beam pipe centre up to 60 mm[1]. The resulting values are scaled to the corresponding proton energy in the case of lower beam energy.

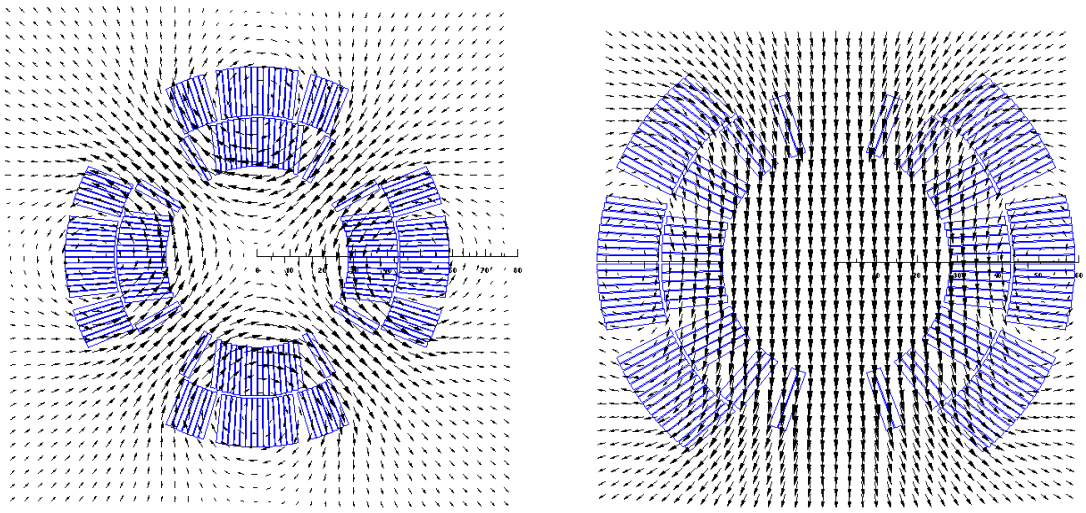

Fig. 3. 2-D field map in main magnets. Left: MQ, right: MD. The field data are used up to 60 mm. The map in MQ is showed beyond 60 mm to show the field structure in the coils.

We will see later on that, the effect of the magnetic field, mainly in the MD is very important. The field bends charged particles, increasing their pathway and consequently, the number of interactions and, so as, the number of secondaries.

[1] This extension is enough for taking into account the effect of the magnetic field

The magnetic field in the MD is opposite in both beam pipes whereas, the magnetic field in the quadrupoles is the same in the twin apertures.

3.3. Point loss initial conditions and loss detection outside the cryostat

The point loss is produced in the arc half-cell when the MQ is focusing, that is when the ß function is at his maxima in the center of the MQ. In consequence the loss will occur at the beam screen in the horizontal plane for a horizontally focusing MQ (named QF), and in the vertical plane for a vertically focusing MQ (named QD). Loss may happen on both sides. Thus, a point loss is considered in the horizontal case, for the innermost and the outermost point of the beam screen. Respectively in the vertical case, the loss may happen on the uppermost and the downermost point.

As pointed out before, the proton to be lost hits the beam screen with an incident angle of 0.25 mrad. It has been observed in some cases that, if the interaction point or vertex is situated just on the beam screen surface, the proton may travel quite a distance in the beam pipe before the first interaction with matter takes place[2]. To prevent the displacement of the point loss and the misunderstanding of the results, the vertex is situated within the beam screen. An intrusion of 10 μm in the beam screen is enough to avoid this last problem.

A point loss is considered at the three possible longitudinal positions z = -325 cm, 0 cm, +325 cm. Respectively these positions correspond to the end of the upstream dipole beam screen, the centre of the quadrupole, and the beginning of the beam screen for the downstream dipole. In these positions is where the loss is supposed to have the maximum value. For a loss in any of both beams, the generated cascade is observed in both detectors, the right detector, RD, and the left detector LD, all along the geometrical configuration. So as, we can obtain, in addition to the direct detection, the signal expected in the detector situated at the opposite side of the vessel, the so called 'cross-talk'.

3.4. Geometrical configurations

Given the geometrical setup for the half-cell described in section 3.1, we have to consider the different possibilities present in the future LHC ring. After every interaction point, beams interchange the vacuum pipe; thus we have the posible configurations shown in Fig. 4. In case A and B, the beam on the right beam pipe is going in the +z direction, and the beam on the left beam pipe in the –z direction. It does only change the focalisation of the MQ. For the C and D configurations, the beams sense is inverted and so on, the magnetic field in the MD.

For any of these geometrical configurations, we have considered the point losses in the transversal positions drawn in the figure (see Fig. 4 right cross-sections). And for any of the latter, the three likely longitudinal positions in the arc-cell. The obtained results and their analysis are presented in the next paragraphs.

In the following, we name the different losses attending to the case, A, B, C, D, and the outer, inner or top position in the beam screen, O, I or T respectively. In this way for instance, for the A configuration we can have an AO and AI loss for the right beam and AT for the left beam. In the B configuration, we can have a loss BT for the right beam and a loss BO and BI for the left beam. It is worth to say that, the loss in the bottom of the beam screen is not considered, as it is completely equivalent by symmetry to the top case. Moreover, the longitudinal position of the point loss will be stated by the *z* co-ordinate of the hitting point (vertex), z_v.

[2] This is due to the way GEANT performs the tracking of the particle.

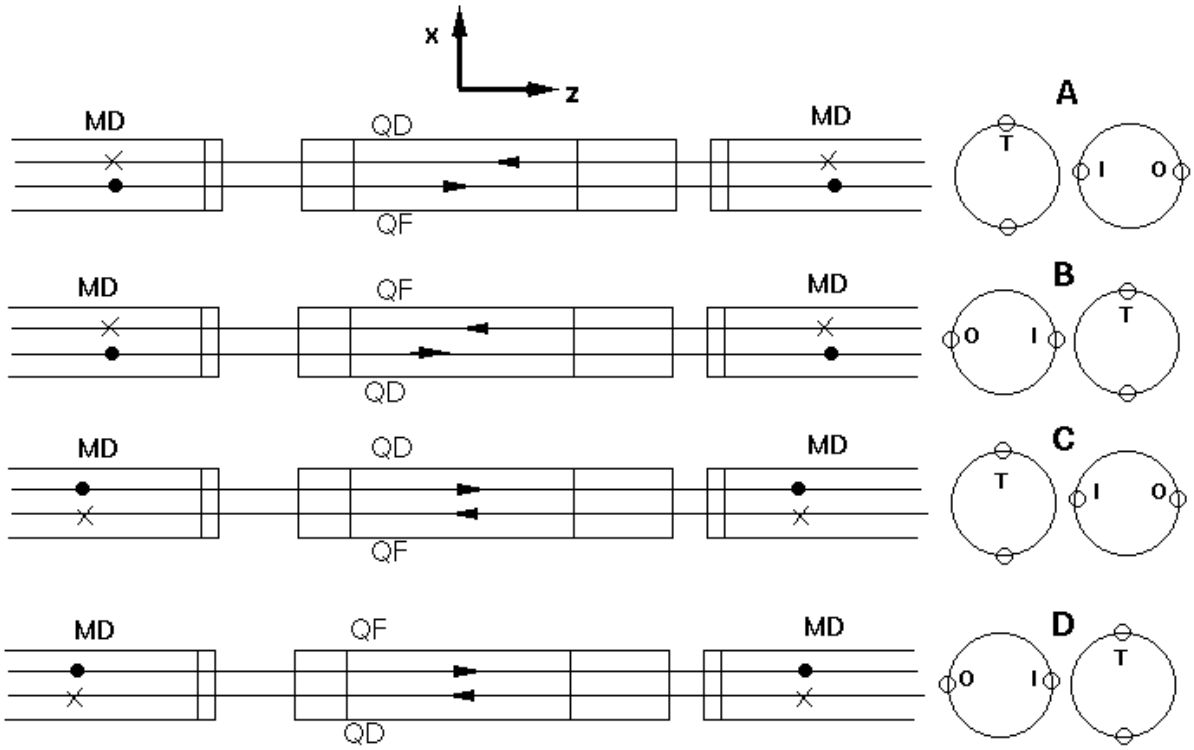

Fig. 4. Schematic representation of the different configurations for the half-cell. View from the top, the arrows mean the direction of the beams. In the MD, the standard signs indicate the magnetic field. In the MQ, QF means focusing and QD defocusing in the horizontal plane. On the right, the different kinds of point losses are shown for each beam pipe; ***T*** *means Top,* ***I*** *means Innermost and* ***O*** *means Outermost.*

4. Results

As a general rule, the shower presents transversally a maximum value in the horizontal plane of the magnet [2]. This is explained because the secondaries have the least amount of material through the way to the detector. On the contrary, the presence of magnetic field gives place to more interactions and more generated secondaries. All this may seem contradictory, but the production of secondaries happens mainly in the first steps, when the particles are very energetic. If too much condensed matter is put in the way out of the secondaries, these are lost in the way and don't reach the detector.

An example of the cascade for the three different longitudinal point losses is shown in Fig. 5. Each histogram represents the longitudinal distribution of generated particles for one point loss.

The observed shower distribution along the beam direction presents the following features:

- The distribution starts approximately at the interaction point, or point loss position.
- It increases sharply to a maximum value, which happens to be between 1 – 2 m from the point loss.

- It decreases softly in the direction of the beam, but it is drastically modulated by the amount of lateral material. As a consequence the distributions present sometimes several secondary maxima.

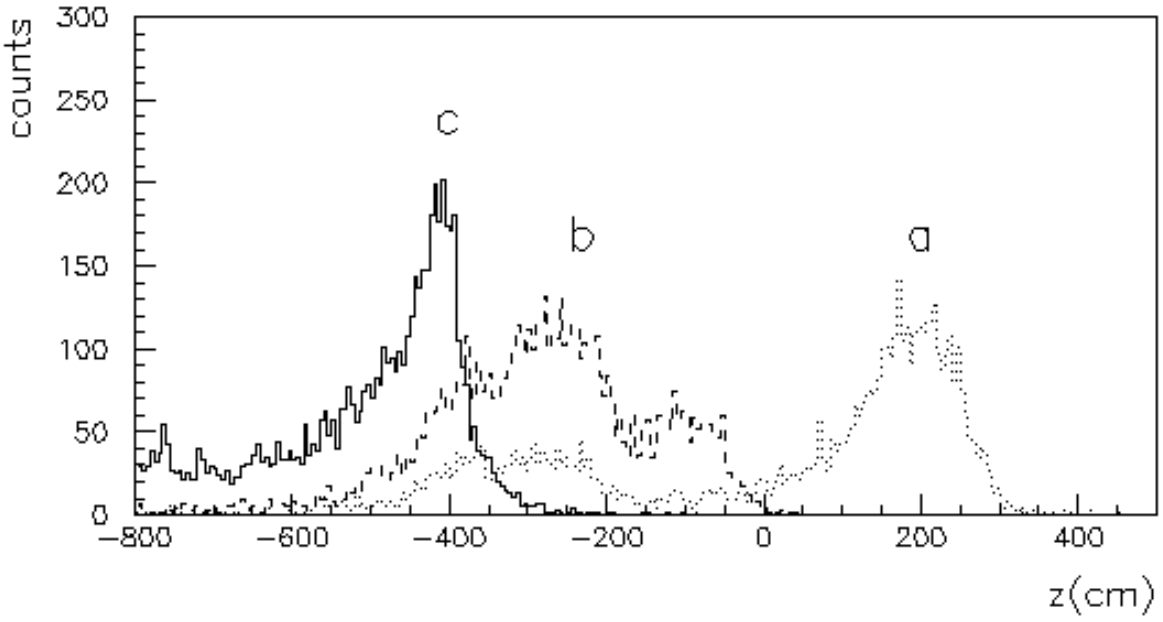

Fig. 5. Developed shower for a point loss in the innermost side of the beam screen, case CI. a) z_v = 325 cm, b) z_v = 0 cm, c) z_v = -325 cm.

To simplify calculations and reduce CPU time, the distribution of secondaries has been created with a hundred protons and with some cuts in the energy. It has been verified that, a hundred protons is enough for obtaining a good statistics in the secondaries distribution. The energy cuts, are used by the program, to stop the tracking of a particle when its energy is under this level. This limit serves also as a detection limit for the detector. All the particles, which have been followed in their track until the detector, have to be at an energy over the cut level. The energy cuts are 0.3 MeV for $e^{\pm}$ and 3.0 MeV for charged hadrons and muons.

The detection is made counting the particles which cross the detector as a function of their position and angle. The angle is calculated between the momentum and the position vector, that is, is the angle of the velocity with the shortest pathway. In some cases, the time of flight is also contabilised in order to obtain the cascade developing time.

The original estimations were made for a point loss of protons in the beam screen, but in some examples, the longitudinal loss distributions have beam integrated to give the doses for a linearly decreasing longitudinal loss distribution.

4.1. General remarks

We are going to analyse in detail the results obtained for the different point losses simulated. The aim is to understand the factors that determine the peculiarities of the generated shower. The main systematic features are presented, and the comparison between them will allow to summarise the behaviour of the beam losses.

For every point loss simulated, a scatter plot is given with the counting of the particles in the detector as a function of the longitudinal position and the height. The detector is 10 cm high, and no difference is observed in the distribution of particles along the height. In general, a projection of the counts into the longitudinal axis is made. The length binning is of 5 cm. In general, a hundred of protons are generated. To obtain the number of particles hitting the detector per squared centimetre and per proton, we have to multiply the count number by $2.0 \cdot 10^{-4}$. From now on, we will call the number of particles as the number of Minimum Ionising Particles (MIPs).

As a general result, it is worth to say that, the main signal (maximum number of MIPs to be detected) is obtained when the point loss happens at the end of the upstream dipole beam screen. That is, just in the long intermagnet gap. A similar intensity is only reached when the loss occurs along the dipole but in the innermost side of the beam screen.

The secondary broad peaks observed in the distributions are usually in coincidence with the intermagnet gaps.

Unless the contrary is stated, the study presented is performed for the results obtained for the detector assigned to every beam. It does mean, that for a loss in the right beam, we analyse the loss distribution at the right detector, and for a loss in the left beam in the left detector. The distribution observed on the other side of the vacuum vessel will be taken into account for the analysis of the 'cross-talk'.

4.1.1. Horizontal loss

In the case of a horizontal loss, it is observed that there is a big difference in the results found for the innermost and the outermost point loss. These differences are common for the losses in the same longitudinal position.

For instance, taking any of the cases considered A, B, C or D, we can compare the results for both horizontal losses. This is shown in Fig. 6 for the A configuration. When the loss is located at the end of the upstream dipole, and beyond, when the cascade is developed in the intermagnet gap, or "matter hole", the intensity is lower for the innermost loss. The same is observed for the first peak of the distribution when the loss is located in the centre of the MQ. This first peak is situated longitudinally in the MQ. The second peak, which is situated in the second intermagnet gap, is practically not affected. Finally, for the loss in the beginning of the downstream dipole, the intensity is amazingly increased for the innermost loss as compared to the outermost loss. It is worth to remember that the shower is developed in the MD.

This behaviour is systematically repeated in all the cases. For the innermost loss, particles have to cross the beam pipe, or in general, they have to travel more distance to get to the detector. Moreover, the incidence angle in the beam screen is opposite in both cases, which would imply a lower number of particles in the detector in the innermost case. To explain the case of the loss along the dipole, we have to make use to the difference in the magnetic map inside the magnets.

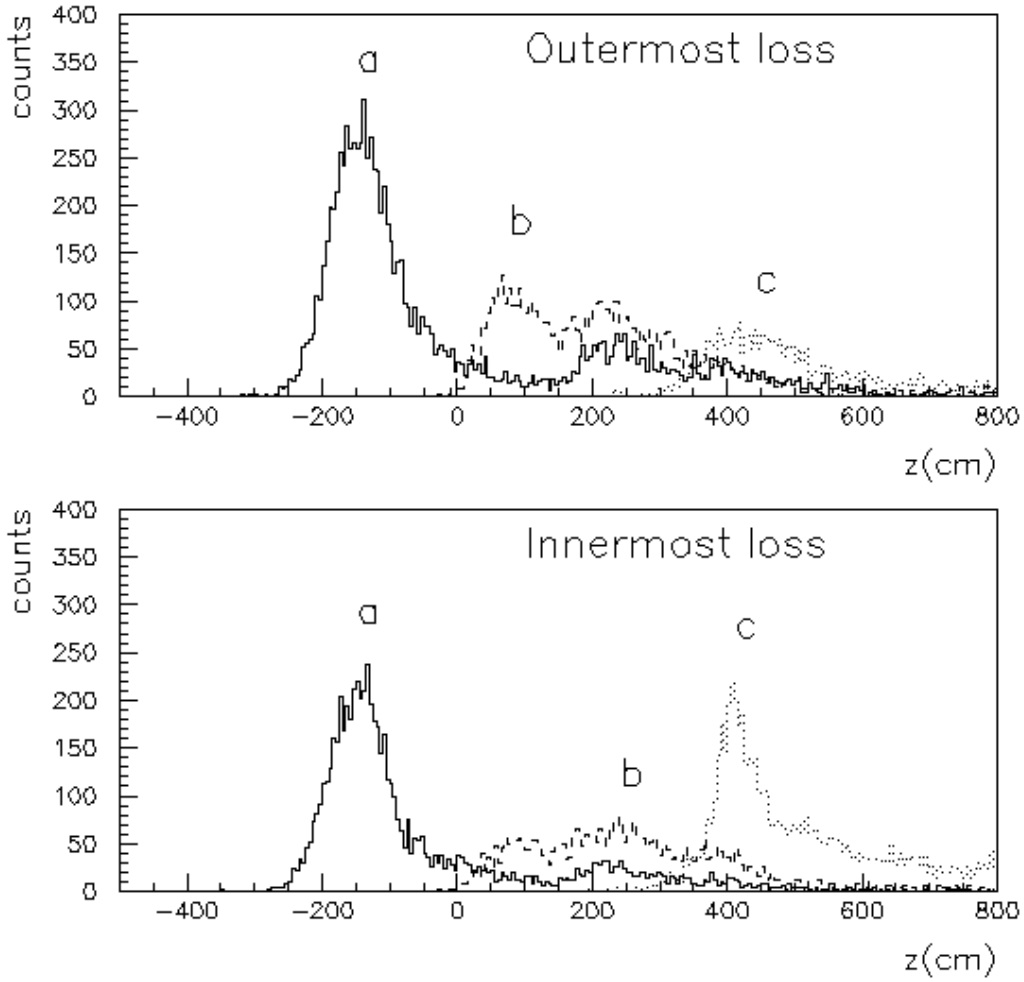

Fig. 6. Example of the differences observed in the horizontal loss. Top figure shows AO results (or outermost loss) and bottom figure the AI results (innermost loss). a) z_v = -325 cm, b) z_v = 0 cm, c) z_v = 325 cm.

4.1.2. Vertical loss

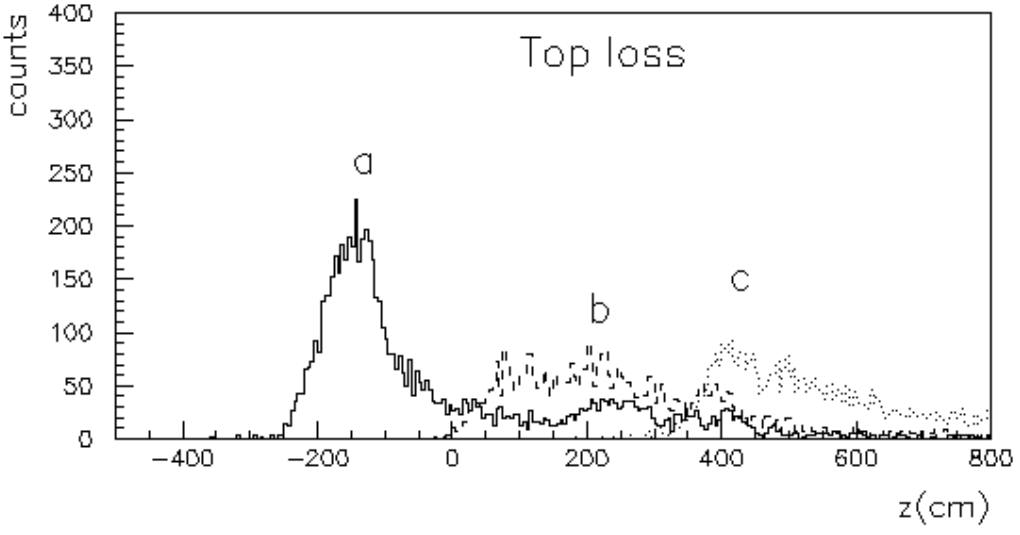

Fig. 7. Example of the three longitudinal losses for a top loss. Case BT.

When the proton is lost in the vertical plane, the top and bottom losses present the same symmetry. Anyway, both cases have been simulated and there exists always a complete similarity between them. Thus, we are going to analyse the unique case of a top loss, or an uppermost point loss. We can see an example in Fig. 7, where it is plotted the results for the B configuration.

As compared with the distributions in the horizontal plane, the results are very similar to that found for the innermost loss when the proton is lost in the upstream MD or in the MQ. In the case of the loss in the downstream dipole, the distribution is very close to that found for the outermost loss.

The explanation can be the same as stated before for the horizontal innermost loss. In this case, for the loss in the dipole, the particles hardly traverse the beam pipe and so as, they hardly feel the magnetic field.

4.1.3. Orientation

For every particle at the detector, the code provides the angle of the particle momentum with its vector position, θ. The origin of the position vector is taken from the point loss vertex, or origin of the cascade. The recovered data gives an idea of the directionality of the cascade. If there exists a preferred orientation, this could determine the orientation of the loss detectors, in order to recover a maximum amount of particles from the generated shower.

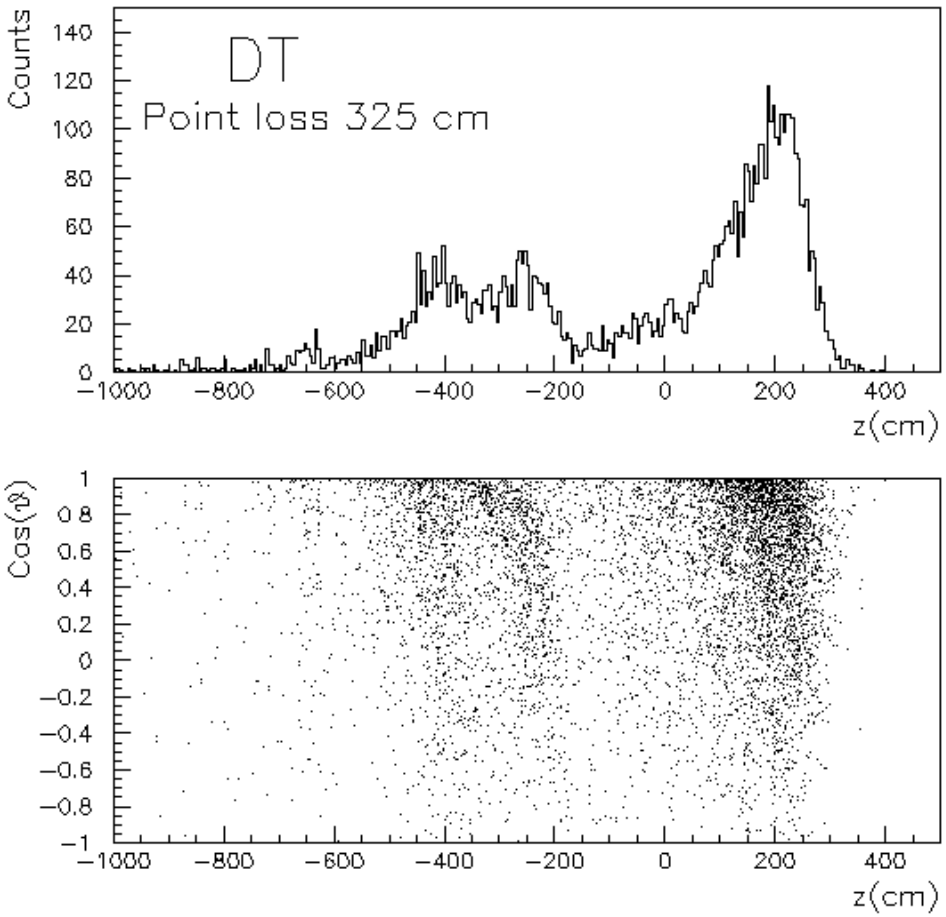

Fig. 8. Top figure: longitudinal distribution of the cascade generated for a DT point loss at z_v = 325 cm. Bottom figure: scatter plot showing cos(θ) as a function of the detector position. θ is the angle between the momentum and the position vector of the particle (the origin is the hitting point).

In the analysis performed, we did not find any orientation for the cascade. The angle spectrum is very wide, showing that particles reach the detector from an extensive range of positions. An example can be seen in Fig. 8 where the shower and the corresponding cos(θ) distribution have been plotted.

Therefore, the detectors will be placed as it has been assumed in the simulations, parallel to the beam.

4.1.4. Cross talk

In order to analyse the cross talk, we look at the signal obtained in the detector assigned to one beam, due to a loss occurring in the other beam.

It is observed mainly one case presenting a non-negligible signal (over the noise level) at the other side over the cryostat. This happens when the cascade is carried over the first intermagnet gap. The intensity is much lower when the cross talk is produced in the second intermagnet gap, which is shorter. In the defined geometrical configuration we can see, that the first gap is about 115 cm whereas the second one is of about 50 cm wide.

In the cases where the intensity is the higher, the cross talk peaks up to a 25% of the intensity observed in the 'true' detector. The values to analyse will be the values of the suitable position for the loss detectors, as there will not be a continuous loss detector all over the half-cell like in the simulations. This study is made later in section 5, where it is proposed the configuration for the loss detectors.

In Fig. 9 is showed an example of the cross-talk in the first intermagnet gap. The direct detection is taken in the left detector (LD), and the cross-talk observed in the right (RD) is about a factor 10 smaller.

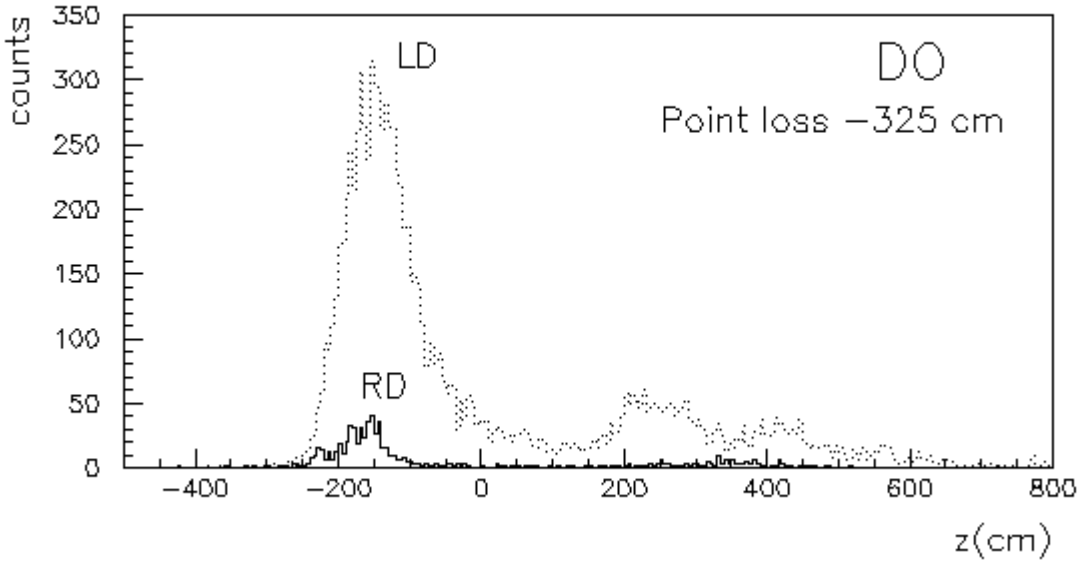

Fig. 9. Example of the cross-talk effect. Point loss in the left beam, case DO. The dotted line represents the signal in the left detector (LD) and the continuous line the signal in the right detector (RD).

4.1.5. Variations with proton energy

Most of the simulations have been done for 7 TeV energy protons, for which a big loss and the immediate energy dose deposition along the superconducting magnets have more drastic effects. To check the influence of the energy in the loss detection, in some cases, it has been obtained the MIPs distribution for energies from 1 – 7 TeV. Moreover, for a high enough number of lost protons, quenching may also occur at injection energy (see Chap. 2).

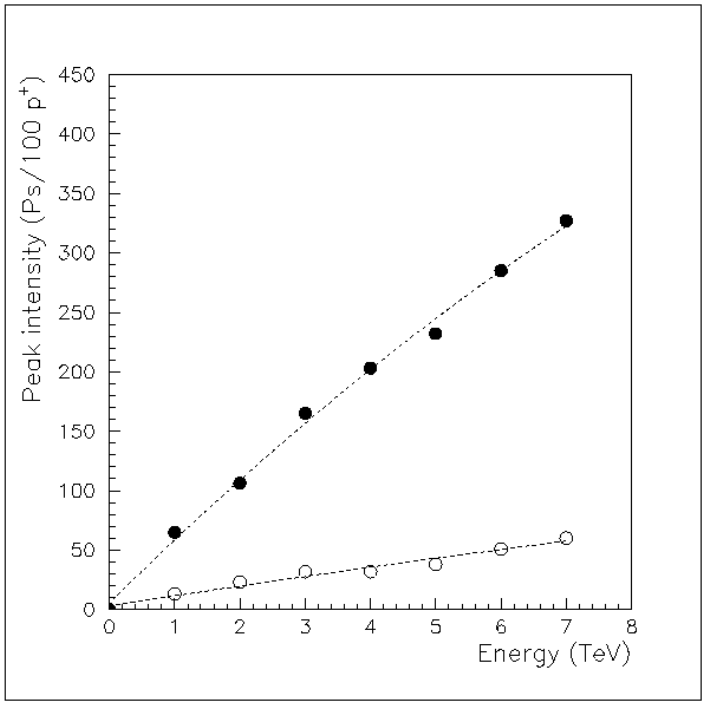

Fig. 10. Evolution with energy of the shower peak for a point loss. Case represented AO. Black points represent the direct detection signal and white points show the cross-talk.

It is found that the shape and position of the MIPs distribution does not present noticeable changes with proton energy. The intensity variation is almost linear with energy. In Fig. 10 is drawn the dependence of the distribution maximum on the beam energy for a point loss of type AO. Similar dependencies have been found in the other considered cases.

4.1.6. Time of flight

After the first interaction, the generated particles travel through the different materials interacting in their turn and creating new secondaries. The arrival time at the detector from the zero time is recorded, so that the shower time of flight can be determined.

The main peak in the distribution corresponds to particles arriving very soon at the detector, as the position is closer to the point loss. The range of time covering the main peak is the time we are interested in. We have considered losses in the three longitudinal positions in the half-cell. In all these cases the time taken by the particles to reach the loss detector ranges from 5 ns to 10 ns. Higher times correspond to the tail of the distribution or to the secondary peaks.

Once the loss detector positions are determined, the time of flight for the shower detected can be determined with a good accuracy in the case of a point loss. For a loss distributed over 4 m, the time of flights are also distributed.

An example of the time of flight and time distribution is shown in Fig. 11. For a point loss we obtain the developed longitudinal shower and the time of flight. In the top figure we can see the longitudinal distribution of particles, and in the middle it is represented the time of flight for every particle as a function of the detector position. It can be seen a straight line which corresponds to the speed of light, or beam speed.

The time distribution for a distributed loss can be estimated computing the time spread of the main peak in the top figure. For this, we take the first 4 m of the longitudinal shower. The difference between the time taken for every particle to reach the detector and the time taken by the beam give us the spread in time of a distributed loss. The results are presented in Fig. 11 in the bottom. It can be seen that the distribution width is about 4 ns.

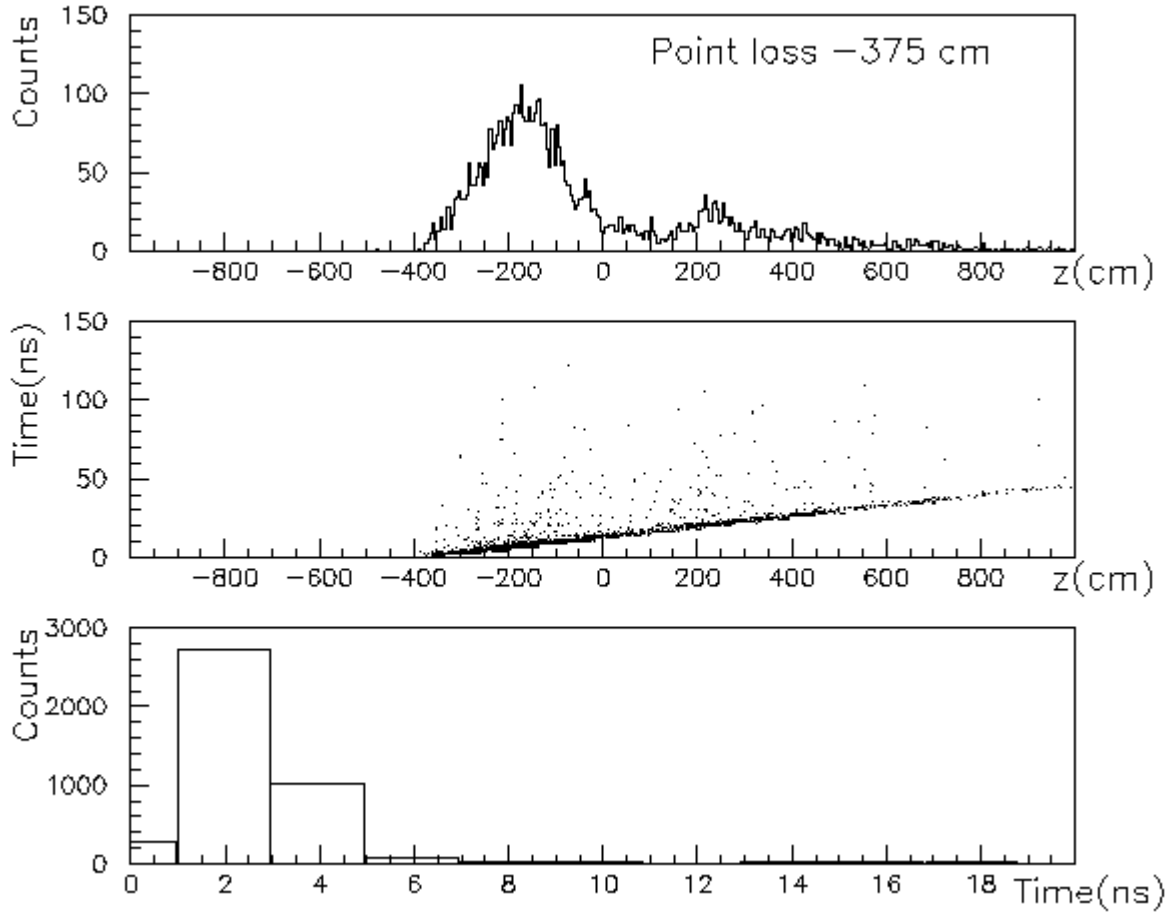

Fig. 11. Representation of particles time of flight. Top figure: shower longitudinal distribution, case BT. Middle: scatter plot showing the time of flight vs. the position. Bottom: time dispersion of the main peak.

4.2. Material and geometry configuration effects

Apart from the effects of the MD magnetic field, the rest of the main characteristics of the particle shower are explained taking into account the geometrical configuration. Moreover, the differences between the several configurations to consider are explained as well due to the matter distribution.

The intermagnet gaps play the main role in the intensity of the cascade. The matter holes act as way outs for the particles, which reach the detector at a further distance than in the case of a shower developed entirely through matter.

In one of the first descriptions of the half–cell used in the calculations, the MD collar were made of aluminium. The MD design was changed putting steel collars instead. In the last version of the geometric description, this has been taking into account. For the point loss in the downstream MD, we find that the number of the MIPs in the detector lows by a factor from 1.4 to 2.0. The different factor corresponds to a different longitudinal position of the point loss. For a top loss the reduction factor is 2.0, 1.6 for an innermost loss and 1.4 for an outermost loss.

When comparing the four geometrical configurations, there exists at its turn, some changes which are caused by the longitudinal asymmetry of the arc-cell. Basically, the first intermagnet gap is twice as long as the second one.

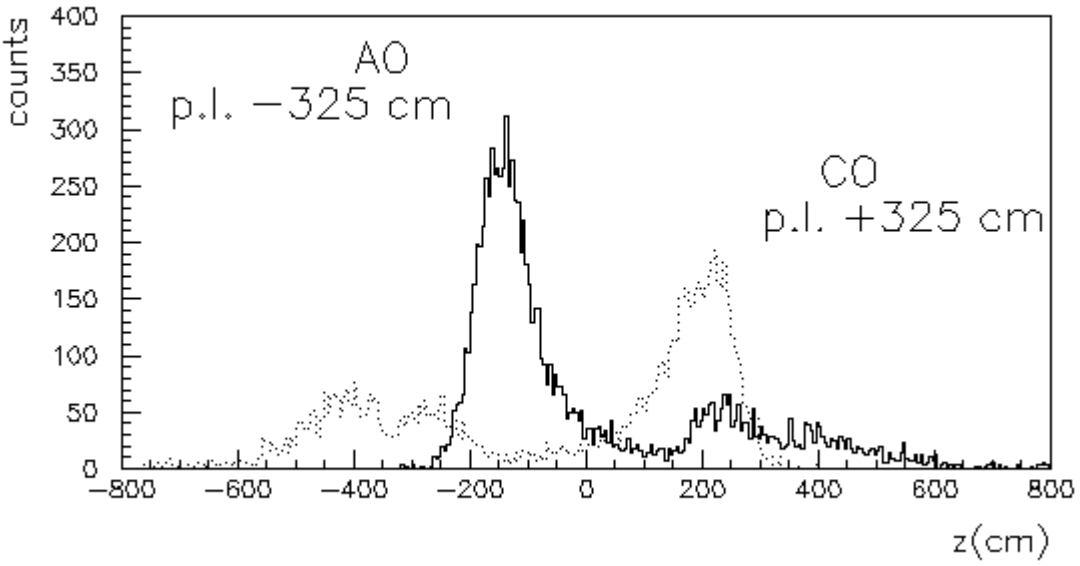

Fig. 12. Showers for two different configurations. Comparison of a loss in the outermost side, AO (continuous line) and CO (dotted line).

In Fig. 12 are showed two examples in which the small differences observed are due to this effect. As a general rule, the distribution caused by a point loss in the upstream dipole is higher in the bigger hole and the maximum is displaced. The intensity of the secondary peaks presents also some variations. In this figure it is represented the losses in the upstream dipole for two opposed beams (case A and C), and for the outermost point loss.

4.3. Magnetic field influence

In previous results [2] it has been found how the magnetic field plays an important role in the energy deposition of high energetic particles in matter. Charged particles are bent by the field, causing to more interactions.

Nevertheless, we have found that this influence is different in the MQ than in the MD. For the losses in the MQ, the observed signal does not change with the magnetic field, even if this one is not considered. On the other hand, the effects of the presence of the bending magnetic field in the MD have found to be of crucial importance.

In order to understand what is happening as the shower is produced in the magnetic materials, it has been used the interactive drawing package of GEANT. This package draws the trajectory of generated particles in the defined geometric set-up. The tracks of particles in the MD are spread horizontally along the magnet coils in a flat spot. If the field is set to zero, the azimutal spreading is uniform.

In the quadrupoles, however, because of the coils symmetry, this azimutal asymmetry in the tracking is not observed.

These results could explain the remarkable increase in the inner lost for the case of the loss in the dipole, what is not reproduced in the MQ.

As an academic test, it has been evaluated the signal to be detected when no magnetic field is applied. The field in the MD increases the intensity by a factor 2 for an outer loss, by a factor 4 for a top loss and a factor 10 in the case of an inner loss.

All in all, the magnetic field in the MD increases the interaction and the secondaries evolution in the mean plane, giving a higher signal when particles have to cross through the magnet material (mainly centred in the beam pipe). In the MQ, the magnetic field may produce an intensifying of the interactions, but the secondaries are spread out homogeneously over the azimutal angle, and no different signal is detected outside the cryostat.

4.4. Longitudinal loss distribution

Up to now, all the results shown were related to point losses. It is worth to evaluate the differences when the case of a distributed loss is considered. For simulating a distribution loss, it is considered that the distribution is triangular in shape (see Fig. 1). A point loss is simulated every 75 cm and the resulting shower is integrated over the loss extension (~ 400 cm). The intensity for every point loss is scaled to the corresponding value in the distribution loss. To compare the results with that of a point loss, the integrated value is scaled to have the total number of loss protons in both kinds of losses.

Distributed losses have been evaluated for the A configuration (see Fig. 4). As the other configurations present quite similar results, the analysis in one configuration can be extrapolated to the other ones. For both beams, a distributed loss can happen for a loss in the upstream dipole and in the quadrupole, whereas a loss in the downstream dipole is a point loss.

Comparing with a point loss, the distribution of particles outside the cryostat for a distribution loss broadens, in general, along the upstream direction. The intensity of the maxima is slightly lower when the loss happens in the quadrupole, or in the dipole for the rightmost hitting point. Nevertheless, the major differences between the shower for the point and the distribution loss occur, when the proton hits the beam screen in the uppermost or the innermost points along the upstream dipole.

It has been evaluated the shower generated for a point loss along the position from the intermagnet MQ-MD to the magnet MD. The distribution loss goes, for instance, from -325 cm to –700 cm. The MD ends at approximately –375 cm. It is found that the shower increases in intensity up to a factor 3 for an innermost loss. The most intense shower is found for a point loss at –400 cm, just inside the magnet. The magnetic field in the magnet beam pipe rises the number of hardronic interactions and the produced secondaries go out into the intermagnet gap.

In Fig. 13 is shown a case in which the differences between the point loss and the distributed loss generated showers are of only 20 %. Nevertheless, in this particular case is when the cross-talk presents the biggest signal. This phenomenon is also expected in a similar way in the D configuration.

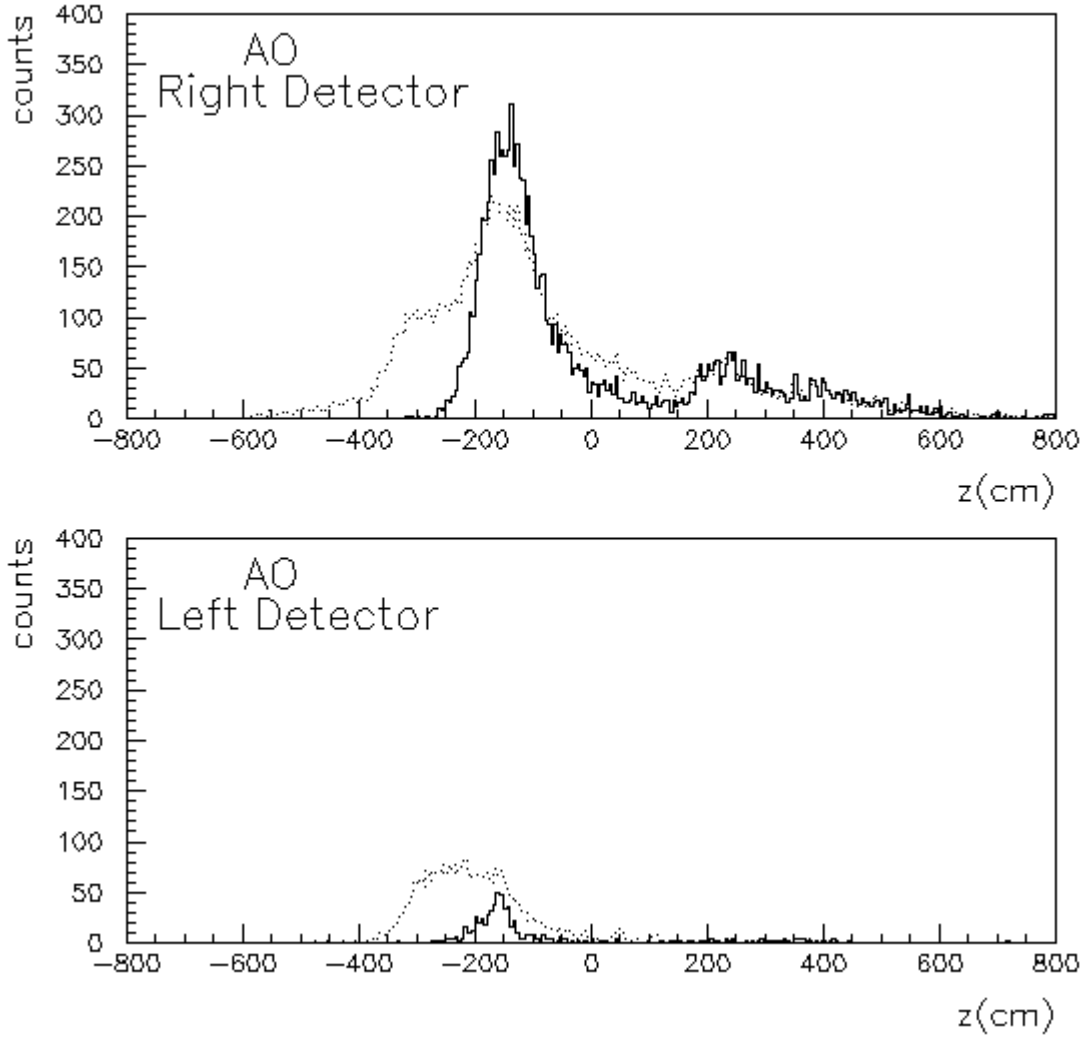

Fig 13. Shower for a point loss (line) and a distributed loss (dots). Case AO, direct detection (top figure) and cross-talk detection (bottom figure). The hitting point is z_v = -325 cm for the point loss, and from –700 cm to –325 cm for the distributed loss.

As for the cross-talk in the case of a distributed loss, that one is not so increased in intensity but in extension as compared to a point loss.

We can conclude that, except for a few exceptions, a point loss is a good approximation for a distributed loss.

5. Position of beam loss detectors

The detection system will be probably made up of PIN diodes. PIN diodes are sensitive to the passage of Minimum ionising particles. For the LHC we need high-speed diodes with a frequency of 40 MHz. The bunch spacing of 25 ns, is a long time compared to the losses mean time, 5 – 10 ns, so as we can measure losses produced in a bunch. Moreover, the measuring system can be synchronised with the passage of the beam.

PIN diode detectors are suitable to have the same threshold for all the positions. We are going to analyse the best configuration for the detection of losses and the detection intensity for the same amount of lost protons.

Table1. Suitable positions for loss detectors and signal observed for every kind of proton losses. In A configuration, results from distributed loss are also presented. For focusing quadrupoles (QF) two signals are listed for innermost and outermost losses.

A	**Right Detector**	*z (cm)*	-150		250		450	
		Intensity(*)	P.l. 260/220	D.l. 210/440	P.l. 70/60	D.l. 70/50	P.l. 60/105	
		Cross-talk(*)	---	---	---	---	---	
	Left Detector	*z (cm)*	-450		-250		200	
		Intensity(*)	P.l. 50		P.l. 105	D.l. 75	P.l. 120	D.l. 150
		Cross-talk(*)	---		10	70	---	---
B	**R D**	*z (cm)*	-150		220		450	
		Intensity(*)	180		70		60	
		Cross-talk(*)	10		10		---	
	LD	*z (cm)*	-450		-250		200	
		Intensity(*)	120/50		120/130		120/170	
		Cross-talk(*)	---		---		---	
C	**RD**	*z (cm)*	-450		-250		200	
		Intensity(*)	60/115		110/110		160/120	
		Cross-talk(*)	---		---		---	
	LD	*z (cm)*	-150		220		450	
		Intensity(*)	180		60		60	
		Cross-talk(*)	10		10		---	
D	**RD**	*z (cm)*	-450		-250		200	
		Intensity(*)	70		110		100	
		Cross-talk(*)	---		10		---	
	LD	*z (cm)*	-150		250		450	
		Intensity(*)	220/290		70/110		100/50	
		Cross-talk(*)	---		---		---	

(*) $\times 2.0 \cdot 10^{-4}$ MIPs/cm^2 per lost proton on the beam screen

The positions for the beam loss detectors have been chosen taking into account several factors. Firstly, when the loss occurs in the horizontal plane, it can not be distinguished if the loss happen in the innermost or in the outermost side of the beam screen. The intensity of the shower at these two points results to be different for most of the cases. Secondly, the detector must be close to the shower longitudinal distribution maximum, so that, the signal to noise ratio is good enough. Finally, the variation of the shower computed for a point and a distributed loss has to be taken into account.

The position for the loss detectors as well as the detection efficiency for the different losses is showed in Table1. For every configuration, the shower intensity is given for a point loss, for the horizontal (two values) and for the vertical losses. The values for the detector corresponding for each beam are given, as well as the 'cross-talk', or value, which can be observed at the detector position for a loss of the same intensity occurring in any point of the other beam. In the case of configuration A, the results of simulations in the case of a distributed loss are shown. The loss may be distributed in the case of a loss in the upstream dipole and in the quadrupole. The computations have been done for a distributed loss over 4 m. As the results for a point loss in the four configurations considered are very similar, the results in Table 1 for a distributed loss can be extrapolated for the other configurations.

It has to be noticed there is only one case in which the direct signal and the cross-talk are at the same level. This has been the example represented in Fig. 14. To have these both signals in the detector it is needed the following coincidence, which is hardly probable: a loss must happen in the upstream dipole for one beam and at the same time, a loss in the quadrupole must occur in the other beam. The probability of both events is of the order of 10^{-4}.

5.1. Intensity variations

In Table1 are shown the counting values for every detector corresponding to the same proton loss. Thus, it can be observed the dispersion in intensity values between the different kind of losses and for the different detectors.

When a loss is produced in the horizontal plane, the shower intensity produced for a point loss in the beam screen innermost or outermost side differs a lot. The biggest difference appears when the loss is developed through the MD. The intensity for the innermost loss is 2.4 times greater than for the outermost loss. In all the horizontal loss cases, we choose the minimum intensity value as a threshold for the detector.

As for the differences in the values for a point/distributed loss, these are quite low for most of the cases. We can see that, in most of the cases, the intensity for a distributed loss is within a 30% similar to the intensity value for a point loss. Again, we find a disagreement for one of the losses. When the loss is distributed along the main dipole, the developed shower is much higher and wider than the corresponding to a point loss. The intensity values in the detector doubles for the distributed loss. As before, we take the minimum between the point loss and the distributed loss as a reference. It is worth to point out that, the distributed loss has been calculated considering a triangular distribution over four meters. In a general case, we can have distributed losses of a more general distribution function and with a different extension.

Once the minimum values are chosen for every detector, these are put together in Table 2. There we have got the threshold for every detector in every configuration for the LHC arcs. The threshold values obtained go from a minimum of 50 up to a maximum level of 220.

Table2. Positions and threshold values for the different loss detectors configurations.

A	**Right Detector**	*z (cm)*	-150	250	450
		Threshold$^{(*)}$	210	50	60
	Left Detector	*z (cm)*	-450	-250	200
		Threshold$^{(*)}$	50	75	120
B	**R D**	*z (cm)*	-150	220	450
		Threshold$^{(*)}$	180	70	60
	LD	*z (cm)*	-450	-250	200
		Threshold$^{(*)}$	50	120	120
C	**RD**	*z (cm)*	-450	-250	200
		Threshold$^{(*)}$	60	110	120
	LD	*z (cm)*	-150	220	450
		Threshold$^{(*)}$	180	60	60
D	**RD**	*z (cm)*	-450	-250	200
		Threshold$^{(*)}$	70	110	100
	LD	*z (cm)*	-150	250	450
		Threshold$^{(*)}$	220	70	50

(*) $\times 2.0 \cdot 10^{-4}$ MIPs/cm^2 per lost proton on the beam screen

5.2. Shielding

As stated just before, there is a factor about 4 between the minimum and the maximum loss detector threshold level. For PIN diodes it would be nice to have the same threshold everywhere.

A solution to unify loss detection levels could be to shield loss detectors. In order to analyse this possibility, several simulations have been done using loss detector shields of tungsten or lead metals.

To the geometrical configuration considered up to now, it has been added a rectangular piece made in lead or in tungsten. This piece has got the same height and length that the simulated loss detector and the thickness is varying to observe the shielding effect. The shield is placed next to the detector in the inner part of it. The thickness has been ranged between 2 mm and 16 mm.

As expected, it is observed a more effective shielding with tungsten than with lead. The observed intensity in the detector lows as the thickness is increased, obtaining a similar evolution for injection and top energy. The developed shower does not change in shape for the shielding. The intensity varies linearly with the shield thickness in the calculated range. For a 16 mm shielding we obtain an intensity diminution factor of 4.7 for tungsten, and 2.8 for lead. The needed factor 4 could be achieved with a tungsten shielding of 15 mm.

If we assume a signal level of 50 for all the loss detectors, we have 10^{-2} MIPs/cm^2/p$^+$. As for injection energy protons, the same amount of loss protons gives a signal about 15 times smaller[3], that is $0.67 \cdot 10^{-3}$ MIPs/cm^2/p$^+$. If we consider a PIN diode of 60% efficiency

[3] This value has a r.m.s. of 30%. Depending on the point loss position, this factor varies between 10 and 20.

(0.6 counts per MIP) and an active surface of 2 mm^2, we have a counting of, $1.2 \cdot 10^{-4}$ counts/p^+ for 7 TeV p^+ and of $0.8 \cdot 10^{-5}$ counts/p^+ for 450 GeV p^+.

As it has been stated before, the quench level for medium range losses is of 10^7 for 7 TeV protons, and of 10^9 for 450 GeV protons. The losses occur in a time of about 10 ms. Thus, the loss rate for a quench is of 10^9 $p \cdot s^{-1}$ at top energy, and 10^{11} $p \cdot s^{-1}$ at injection energy. The count rate in the loss detector for a quench would be therefore, 10^5 counts/s and$\cdot 10^6$ counts/s for top and injection energy respectively. We obtain a factor around 10 between the count rate at low and high energy. The quench threshold in the PIN diodes should be modulated with energy while acceleration ramping.

6. Conclusions

We have assumed to have three positions for the point losses around a focusing quadrupole in the SSS of the LHC. The developed shower simulated for a point loss with the code GEANT 3.21 presents the following characteristics:

- The longitudinal distribution of MIPs produced peaks at a distance of 1 – 2 m from the interaction point.
- The differences found in intensity and shape in the several distributions considered can be explained mainly due to the geometric and magnetic field configuration.
- There exist very few cases of 'cross-talk'. It can be stated in which beam the loss is produced.
- The time of flight dispersion of the shower is of 4 ns.

A beam loss detection system has been proposed with a set of six Beam Loss Monitors around each Main Quadrupole. All the possible geometric and magnetic field configurations in the LHC arcs are considered. The BLMs have to be placed outside the cryostat in the medium plane. Three BLMs at each side will measure the beam losses of the respective beam. The exact location is given as well as the threshold level for detection. A common threshold for the BLM configuration is achieved by means of a detector shielding with a tungsten plate 0 – 15 mm thick.

7. References

1. Application Software Group. CERN – CN Division,
   GEANT – Detector Description and Simulation Tool
2. T. Spickermann and K. Wittenburg, Simulation of Point Beam Losses in LHC Superconducting Magnets, LHC Project Note 124, CERN 1997.
3. J.B. Jeanneret et al., Quench Levels and transient Beam Losses in LHC Magnets, LHC Project Report 44, CERN, 1996.
4. C. Bovet and J.B. Jeanneret, Tertiary beam losses in LHC arcs, LHC Project Note 125, CERN 1997.
5. K.M. Potter et al., Estimates of Dose to Components in the Arcs of the LHC due to Beam-Loss and Beam-Gas Interactions, LHC Project Note 18, CERN 1995.
6. K.M. Potter and G.R. Stevenson, Source Intensities for use in the Radiological Assessment of the effect of Proton Losses at the Scrapers and around the Main Ring of the LHC, CERN AC/95-04(DI), CERN/TIS-RP/IR/95-16, LHC Note 322.

7. M. Huhtinen and G.R. Stevenson, Doses around the LHC beam-pipe due to beam-gas interactions in along straight section, LHC Project Note 39, CERN 1996.
8. The Large Hadron Collider – Conceptual Design, CERN/AC/95-05(LHC).